Supporting Information for Readers

Synthesis, crystal structure, and ionic conductivity of hydride ion-conducting Ln_2LiHO_3 (Ln = La, Pr, Nd) oxyhydrides

Yuki Iwasaki,[a] Naoki Matsui,[a] Kota Suzuki,[a,b] Yoyo Hinuma,[c,d] Masao Yonemura,[e] Genki Kobayashi,[f,g] Masaaki Hirayama,[a,b] Isao Tanaka[d,i,h,j] and Ryoji Kanno,[a, b]*

[a] Department of Chemical Science and Engineering, School of Materials and Chemical Technology, Tokyo Institute of Technology, 4259 Nagatsuta, Midori-ku, Yokohama 226-8502, Japan

[b] All-Solid-State Battery Unit, Institute of Innovative Research, Tokyo Institute of Technology, 4259 Nagatsuta, Midori-ku, Yokohama 226-8503, Japan

[c] Center for Frontier Science, Chiba University, 1-33 Yayoi-cho, Inage, Chiba 263-8522, Japan

[d] Center for Materials Research by Information Integration, Research and Services Division of Materials Data and Integrated System, National Institute for Materials Science, 1-2-1, Sengen, Tsukuba 305-0047, Japan

[e] Neutron Science Laboratory (KENS), Institute of Materials Structure Science, High Energy Accelerator Research Organization (KEK), 1-1 Oho, Tsukuba, Ibaraki 305-0801, Japan

[f] Department of Materials Molecular Science, Institute for Molecular Science, National Institute of Natural Sciences, 38 Nishigonaka, Myodaiji, Okazaki, Aichi 444-8585, Japan

[g] SOKENDAI (The Graduate University for Advanced Studies), 38 Nishigonaka, Myodaiji, Okazaki, Aichi 444-8585, Japan

[h] Department of Materials Science and Engineering, Kyoto University, Kyoto 606-8501, Japan

[i] Center for Elements Strategy Initiative for Structure Materials (ESISM), Kyoto University, Kyoto 606-8501, Japan

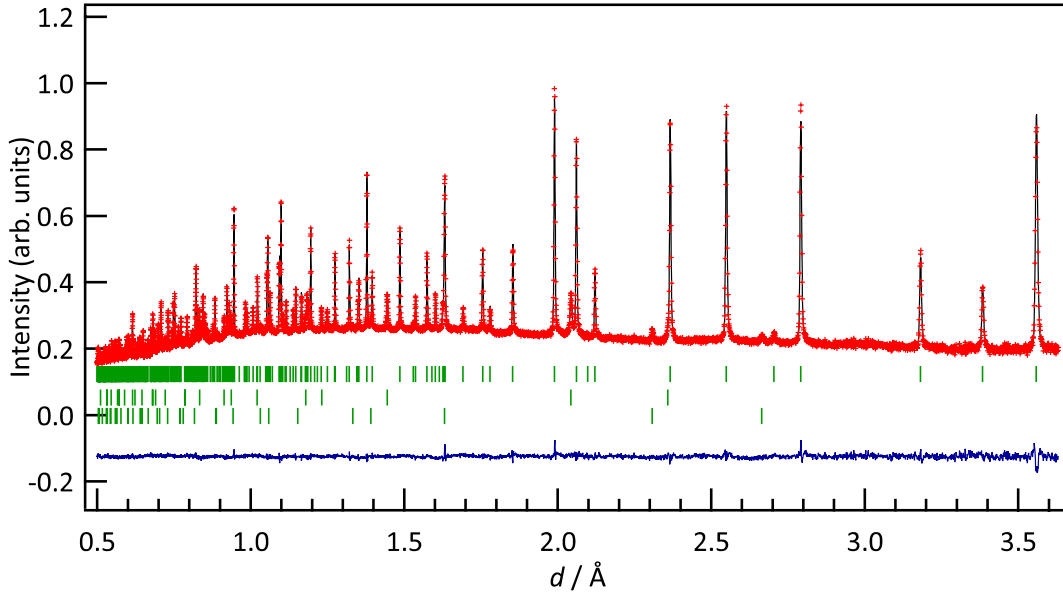[j] Nanostructures Research Laboratory, Japan Fine Ceramics Center, Nagoya 456-8587, Japan

Figure S1. Neutron Rietveld refinement results for Pr_2LiHO_3. The observed, calculated and residual differences are denoted by the red crosses, a black line and a blue line, respectively. The green tick marks indicate the positions of Bragg reflections.

Table S1. Rietveld refinement results from the Pr_2LiHO_3 NPD spectrum at 298 K.

Atom	Site	g	x	y	z	B_{iso} / Å^2	U_{11} / Å^2	U_{22} / Å^2	U_{33} / Å^2
Pr(1)	$4i$	0.997(12)	0	0	0.362185(19)	0.503(7)	0.00597(18)	0.00814(19)	0.0050(2)
Li(1)	$2a$	1	0	0	0	1.00(3)	0.0112(7)	0.0037(6)	0.0230(10)
H(1)	$2b$	0.9783(13)	0.5	0	0	1.55(2)	0.0175(5)	0.0171(5)	0.0244(6)
O(2)	$2b$	=1−g[H(1)]	0.5	0	0	=B[H(1)]	=U_{11}[H(1)]	=U_{22}[H(1)]	=U_{33}[H(1)]
O(1)	$2d$	0.9643(13)	0.5	0	0.5	0.417(11)	0.0068(3)	0.0034(3)	0.0057(3)
H(2)	$2d$	=1−g[O(1)]	0.5	0	0.5	=B[O(1)]	=U_{11}[O(1)]	=U_{22}[O(1)]	=U_{33}[O(1)]
O(3)	$4i$	1	0	0	0.17745(3)	0.653(7)	0.01064(18)	0.00957(18)	0.00461(18)

Unit cell: orthorhombic *Immm* (71); a = 3.510221(10) Å, b = 3.707429(10) Å, c = 12.7269(3) Å, V = 165.6267 Å^3; R_{wp} = 1.70%, R_e = 1.07%, R_p = 1.45%, R_B = 4.03%, R_F = 4.74%, goodness of fit $S = R_{wp}/R_e$ = 1.59; and secondary phase: LiH (~1.2 mass%) and ternary phase: Li_2O (0.4 mass%).
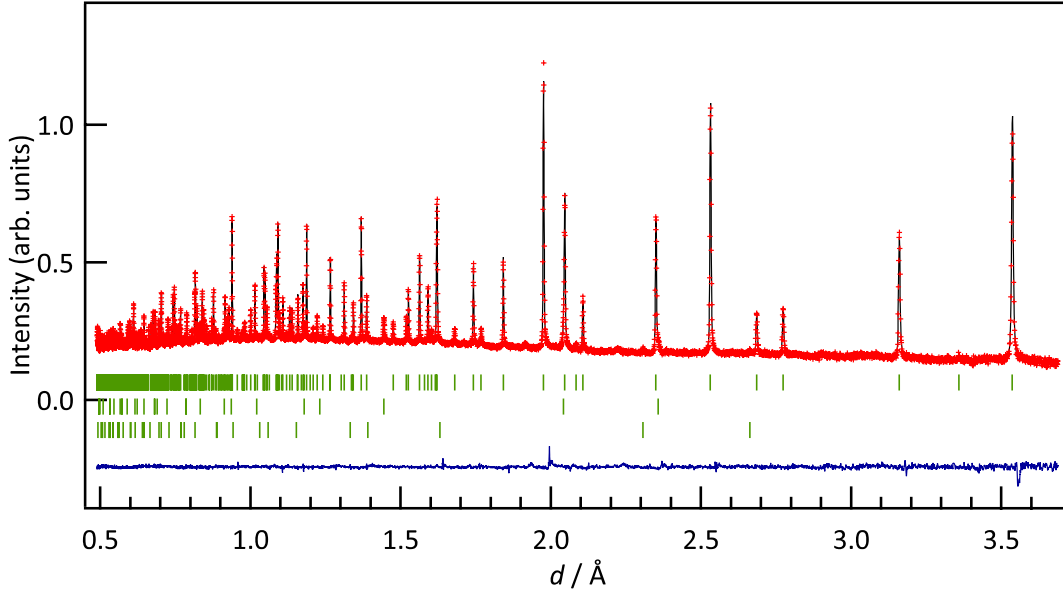
Figure S2. Neutron Rietveld refinement results for Nd_2LiHO_3. The observed, calculated and residual differences are denoted by the red crosses, a black line and a blue line, respectively. The green tick marks indicate the positions of Bragg reflections.

Table S2. Rietveld refinement results from the Nd_2LiHO_3 NPD spectrum at 298 K.

Atom	Site	g	x	y	z	B_{iso} / Å²	U_{11} / Å²	U_{22} / Å²	U_{33} / Å²
Nd(1)	$4i$	0.9914(12)	0	0	0.36355(2)	0.210(4)	0.00258(9)	0.00381(10)	0.00158(9)
Li(1)	$2a$	1	0	0	0	0.89(2)	0.0086(7)	0.0065(7)	0.0187(9)
H(1)	$2b$	0.993(3)	0.5	0	0	1.889(18)	0.0188(5)	0.0226(5)	0.0304(6)
O(1)	$2d$	0.9519(9)	0.5	0	0.5	0.326(7)	0.0052(2)	0.0029(2)	0.0042(2)
H(2)	$2d$	$=1-g[O(1)]$	0.5	0	0.5	$=B[O(1)]$	$=U_{11}[O(1)]$	$=U_{22}[O(1)]$	$=U_{33}[O(1)]$
O(3)	$4i$	1	0	0	0.17703(3)	0.598(6)	0.01009(16)	0.00812(16)	0.00451(14)

Unit cell: orthorhombic *Immm* (71); a = 3.485429(8) Å, b = 3.684503(8) Å, c = 12.64382(3) Å, V = 162.3729 Å³; R_{wp} = 1.87%, R_e = 1.20%, R_p = 1.58%, R_B = 2.77%, R_F = 3.49%, goodness of fit $S = R_{wp}/R_e$ = 1.56; and secondary phase: LiH (~1.6 mass%) and ternary phase: Li_2O (0.2 mass%). The g in H(1) is very close to 1, and the non-existence of the vacancies in this site cannot be statistically ruled out.
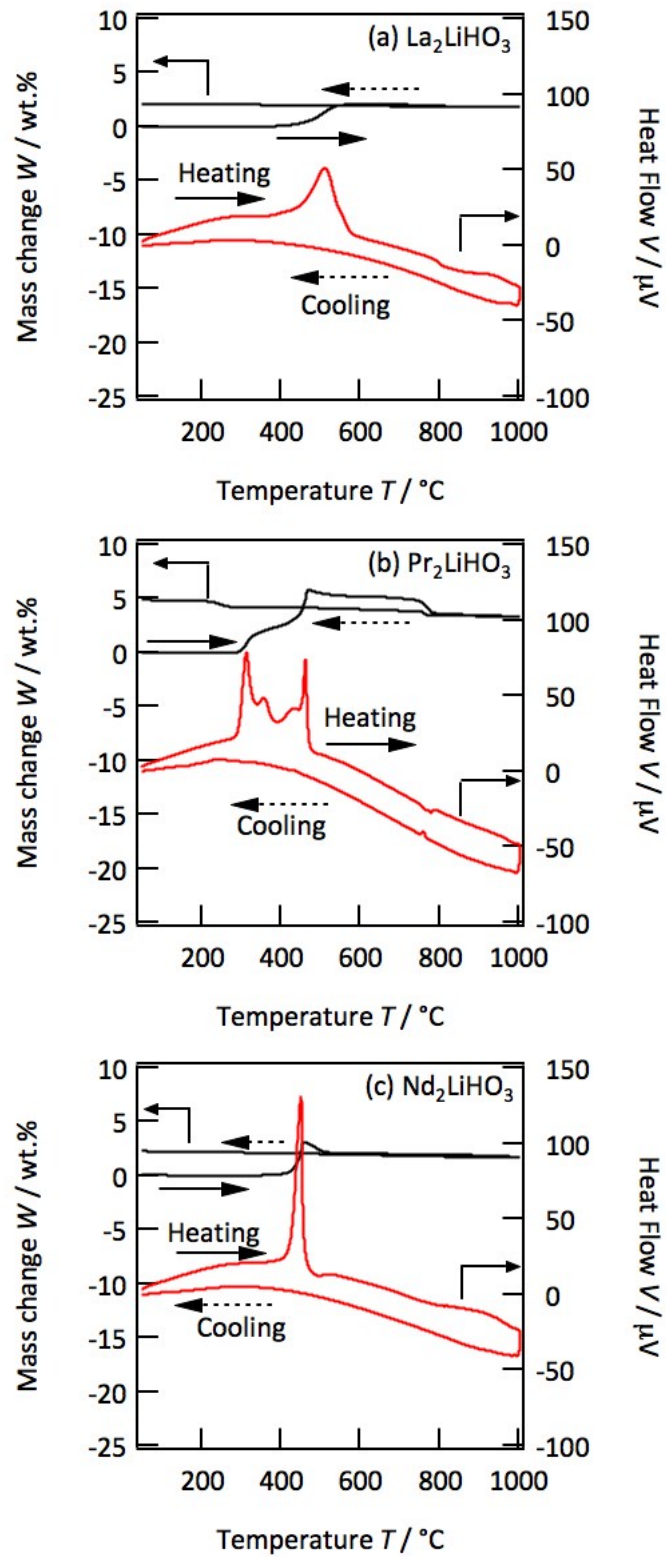
Figure S3. TG/DTA curves for Ln_2LiHO_3 (Ln = La, Pr, Nd) under oxygen gas.
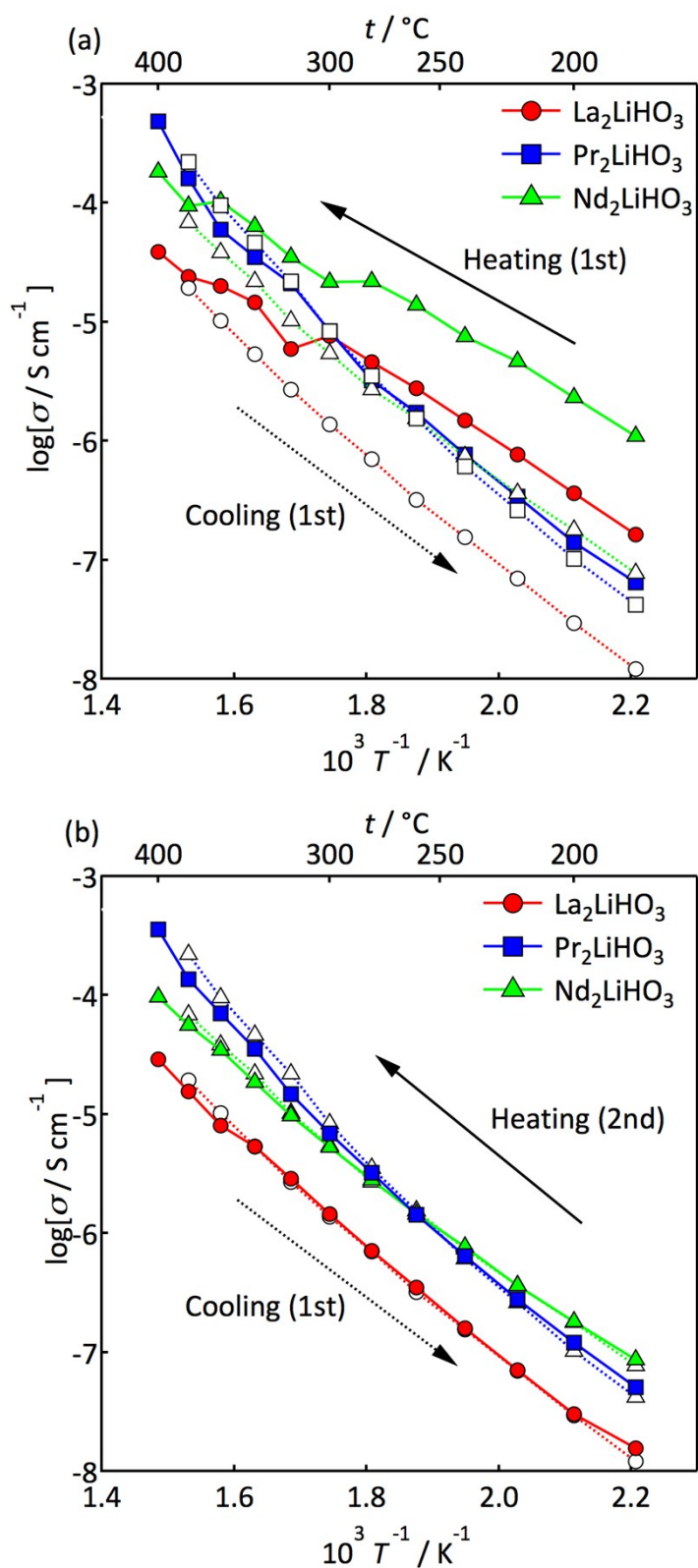
Figure S4. Arrhenius plots of the ionic conductivity of Ln_2LiHO_3 (Ln = La, Pr, Nd) during the (a) first heating and cooling processes and the (b) first cooling and second heating processes.
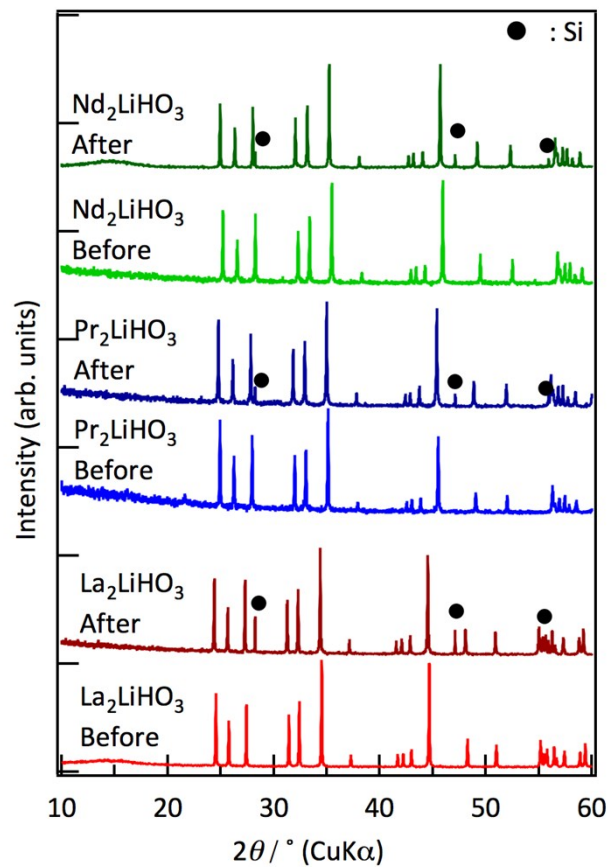
Figure S5. X-ray diffraction patterns of Ln_2LiHO$_3$ (Ln = La, Pr, Nd) before and after the AC-impedance measurements.